Electronic Supplementary Material (ESI) for Journal of Materials Chemistry A.

Supporting Information

Cost-effective fabrication of high-performance flexible all-solid-state carbon micro-supercapacitors by blue-violet laser direct writing and further surface treatment

Jinguang Cai,[ab] Chao Lv[ab] and Akira Watanabe*[a]

[a] Institute of Multidisciplinary Research for Advanced Materials, Tohoku University, 2-1-1 Katahira, Aoba-ku, Sendai 980-8577, Japan
E-mail: watanabe@tagen.tohoku.ac.jp
[b] China Academy of Engineering Physics, P.O. Box 919-71, Mianyang 621900, Sichuan, P. R. China

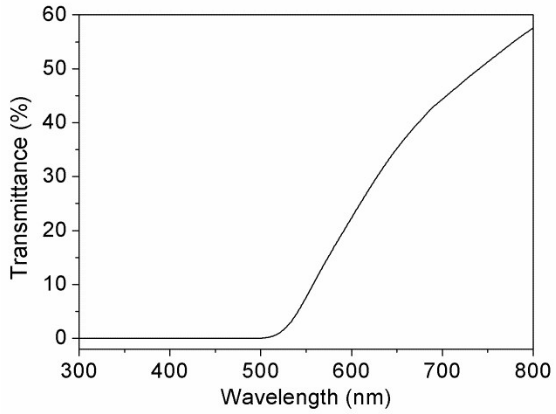

Fig. S1. UV-vis transmission spectrum of PI sheet with a thickness of 125 μm.

Fig. S2. Digital photograph of the adopted 405 nm CW semiconductor laser with high power and small volume.

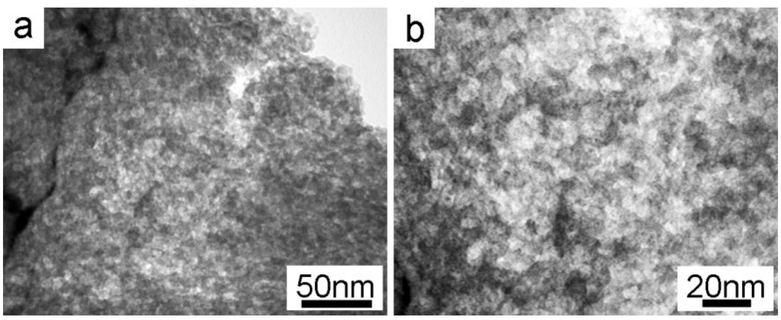

Fig. S3. TEM images of carbon structures obtained by laser writing on PI at laser power of 157 mW.

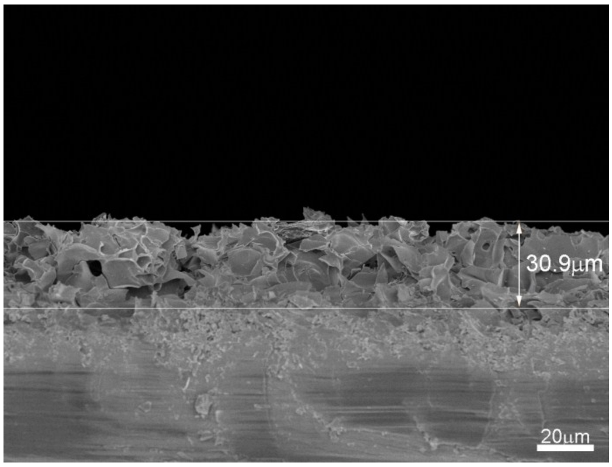

Fig. S4. Cross-section SEM image of carbon structures obtained by laser direct writing at laser power of 157 mW.

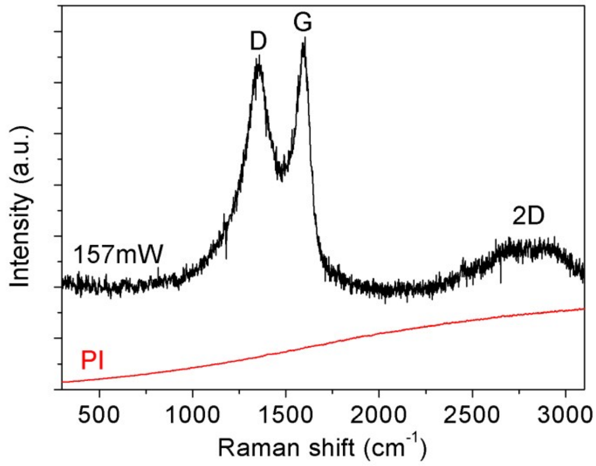

Fig. S5. Raman spectra of LISs at 157 mW and original PI film.

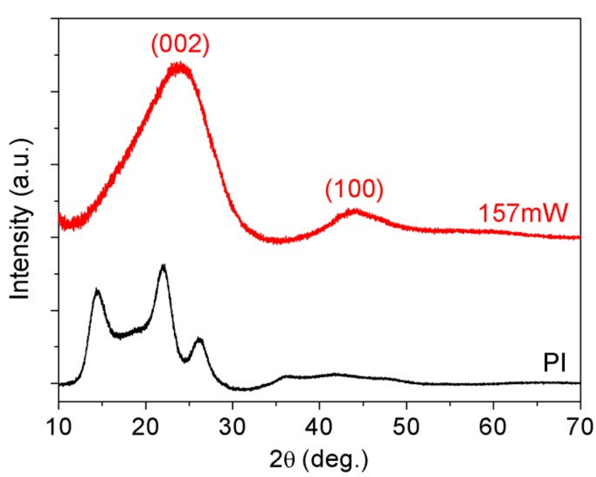

Fig. S6. XRD patterns of powdered LISs scraped from PI sheet and original PI sheet.

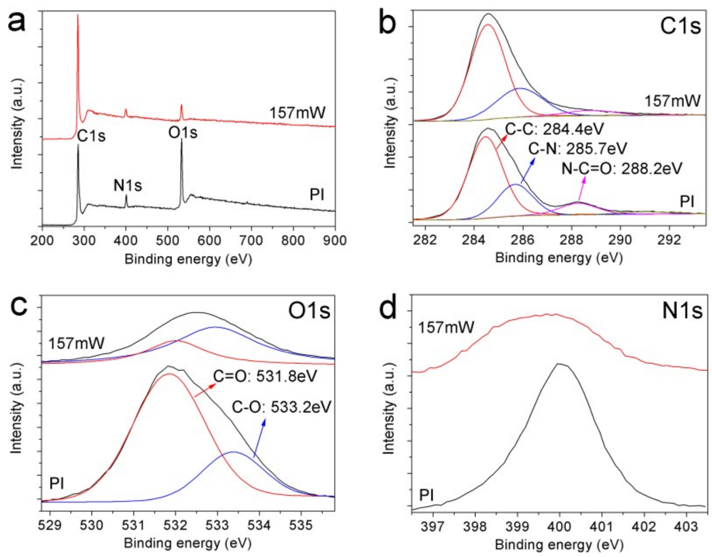

Fig. S7. XPS spectra (a), C1s XPS spectra (b), O1s XPS spectra (c), and N1s (d) of LISs film and original PI sheet.

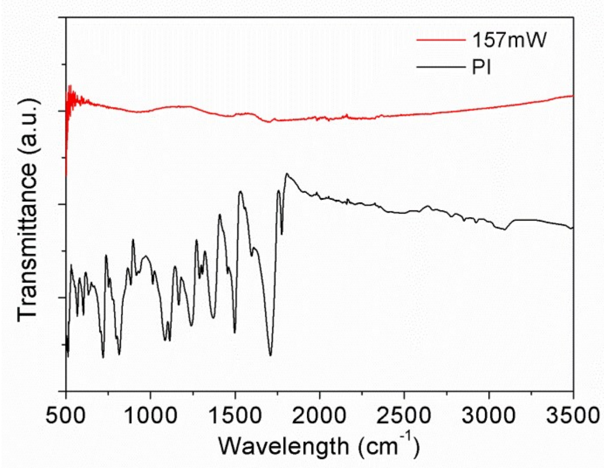

Fig. S8. FT-IR spectra of LISs film and original PI sheet.

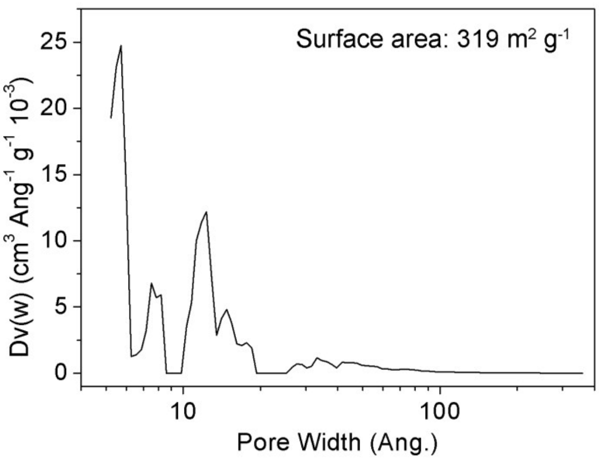

Fig. S9. Pore size distribution of laser induced carbon structures at laser power of 157 mW, which was obtained by density functional theory calculation (Software: Autosorb ver. 1.51, Quantachrome; Model: N_2 at 77K on carbon, slit pore).

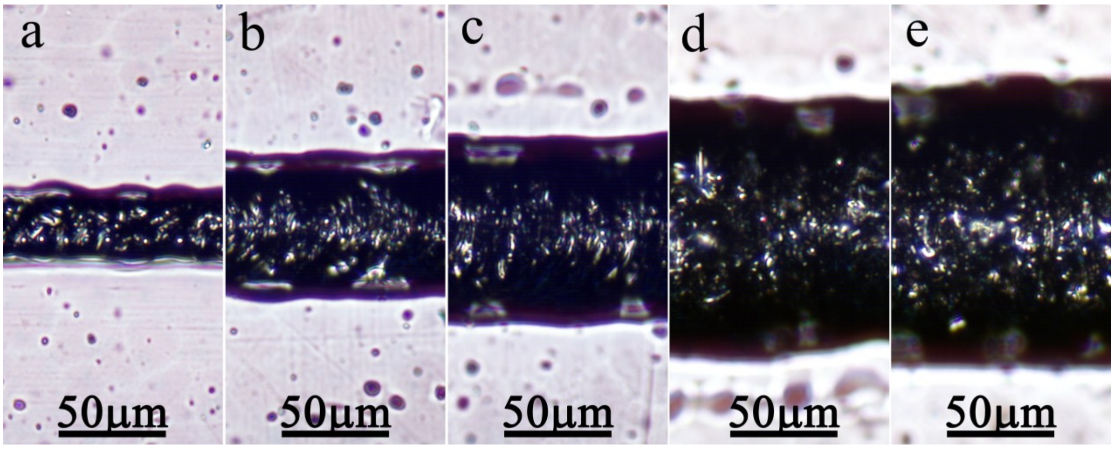

Fig. S10. Optical microscopy images of single lines carbonized by laser direct writing at different laser power. (a) 64 mW, (b) 82 mW, (c) 111 mW, (d) 157 mW, and (e) 218 mW.

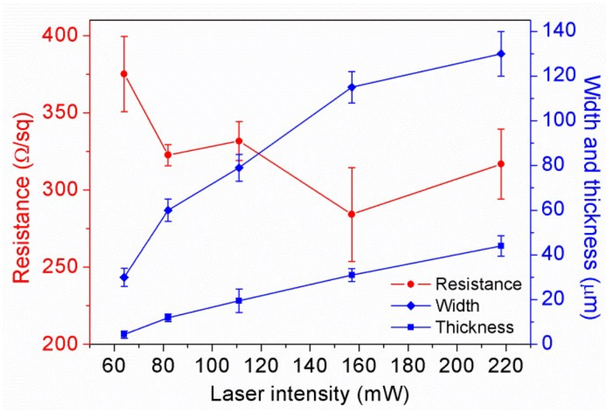

Fig. S11. The resistance and thickness of carbon films and width of single lines obtained at different laser power.

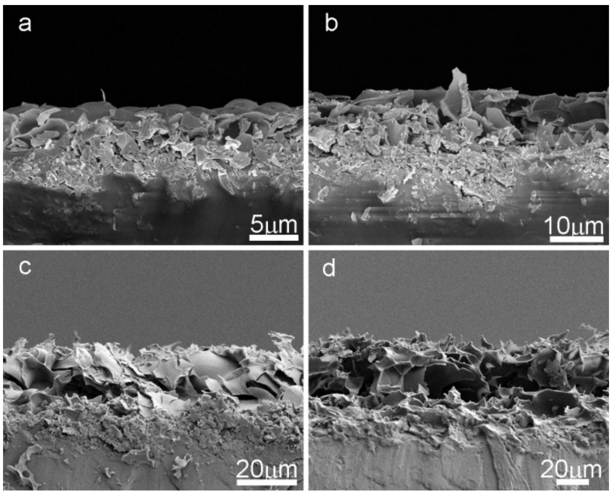

Fig. S12. Cross-section SEM images of carbon structures obtained by laser direct writing at different laser power: (a) 64 mW, (b) 82 mW, (c) 111 mW, and (d) 218 mW.

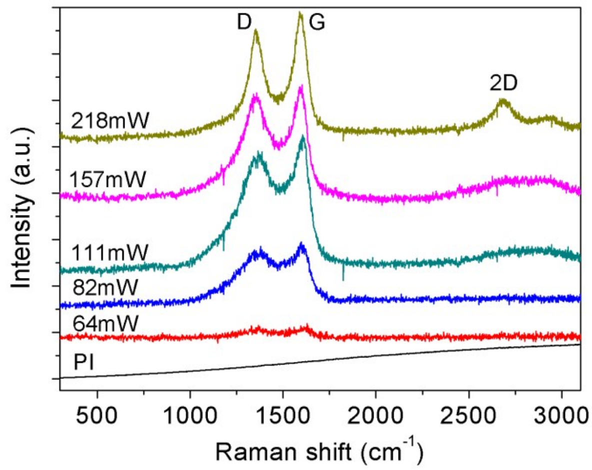

Fig. S13. Raman spectra of original PI film and LISs obtained at different laser power.

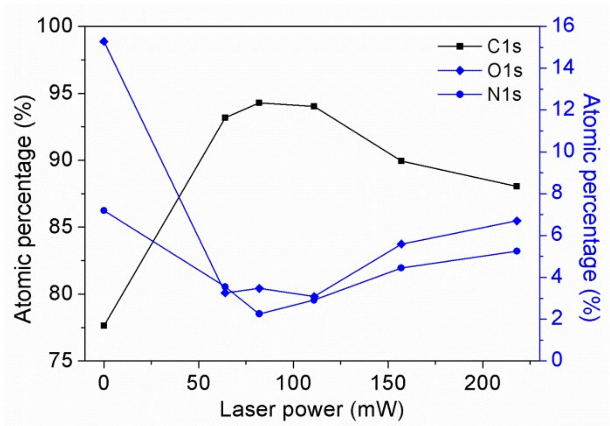

Fig. S14. Atomic percentages of carbon, oxygen and nitrogen obtained from XPS data of the structures prepared at different laser power.

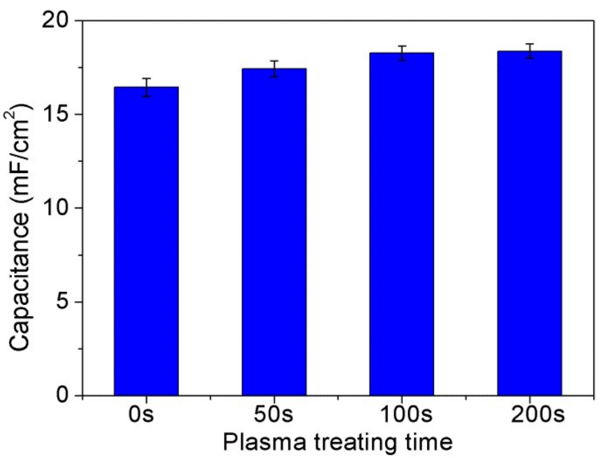

Fig. S15. Specific capacitances calculated from CV curves of MSCs obtained at laser power of 157 mW after plasma treating for different time. Scan rate is 10 mV/s.

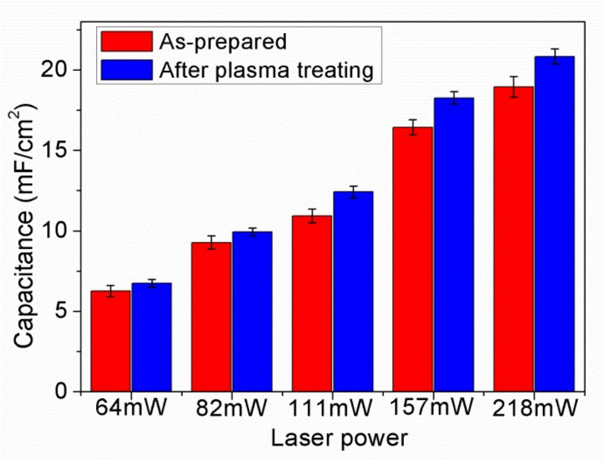

Fig. S16. Specific capacitances of MSCs before and after plasma treating calculated from CV curves as a function of laser power at a scan rate of 10 mV/s.

Table S1. Comparison of specific capacitance (mF/cm^2) of MSCs based on carbon materials

Preparation method [a]	Materials [b]	Electrolyte [c]	Specific capacitance (mF/cm^2) [d]	Ref.[e]
LC	**Carbon**	**PVA/H_2SO_4**	**18.3 @ 10 mV/s** **35 @ 0.05 mA/cm^2**	**This work**
Screen printing	N-doped RGO	PVA/H_3PO_4	3.4 @ 20 $\mu A/cm^2$	19
LC	Carbon	PVA/H_3PO_4	0.8 @ 10 mV/s	40
LIG	Graphene	PVA/H_2SO_4	9 @ 20 $\mu A/cm^2$	37
Photolithography	Carbon onion	Et_4NBF_4/PC	1.7 @ 1 V/s	17
Photolithography	Activated carbon	Et_4NBF_4/PC	11.6 @ 0.5 V/s	17
LIG	B-doped graphene	PVA/H_2SO_4	16.5 @ 50 $\mu A/cm^2$	39
LIG	Graphene	H_2SO_4	4 @ 20 mV/s 3.9@0.2 mA/cm^2	38
Photolithography	MWCNT	Ionogel	~0.265 @ 10 mV/s*	18
Photolithography	RGO	PVA/H_2SO_4	0.87 mF/cm^2 @ 1 V/s	21
Photolithography	Graphene/MWCNTs	PVA/H_3PO_4	2.54 @ 10 mV/s	14
Laser scribing	LSG/MWCNTs	PVA/H_3PO_4	~0.5 @ 0.16 mA/cm^2*	36
Photolithography	MWCNTs	PVA/H_3PO_4	2.75 @ 10 mV/s*	23
Photolithography	Graphene/CNTs	Na_2SO_4	2.16	46
Laser scribing	RGO	PVA/H_2SO_4	2.32 @ 13 $\mu A/cm^2$	35
Laser reduction	RGO	Hydrated GO	0.51 @ 20 mV/s	27
LBL assembly	RGO	PVA/H_3PO_4	~0.4	45
Photolithography	Activated carbon	Et_4NBF_4/PC	2.1	44
Photolithography	CDC	Et_4NBF_4/PC	1.5 @ 100 mV/s	43
Photolithography	RGO/CNT	3 M KCl	6.1 @ 10 mV/s	42
Photolithography	GQDs	0.5M Na_2SO_4	0.534 @ 15 $\mu A/cm^2$	41
Lithography	Graphene	PVA/H_2SO_4	0.0807 @10 mV/s	47
Lithography	MWCNT	PVA/H_2SO_4	0.562@1V/s	48
Photolithography	RGO	PVA/H_3PO_4	0.54@0.5V/s	49
Lithography	SWCNT	H_2SO_4	0.364*	50
Photolithography	Porous carbon	H_2SO_4	0.75@100mV/s	51
Photolithography	Graphene	PVA/H_2SO_4	0.116@10mV/s	52
Photolithography	MWCNT	Ionogel	~0.33@1V/s*	53
Photolithography	RGO	PVA/H_3PO_4	0.462	54
Photolithography	RGO	PVA/KOH	0.897@10mV/s	55
Lithography	BNG	PVA/H_2SO_4	0.39@10mV/s*	56
Lithography	Activated graphene	PVA/H_2SO_4	89.5@10mV/s	57
Photolithography	nc-PDDA-Gr	PVA/H_2SO_4	409	58

[a] Laser carbonization (LC) and laser induced graphene (LIG). [b] Reduced graphene oxide (RGO), multiwalled carbon nanotubes (MWCNTs), carbon nanotubes (CNTs), laser scribed graphene (LSG), carbide derived carbon (CDC), graphene quantum dots (GQDs), single-walled carbon nanotubes (SWCNTs), nitrogen and boron co-doped graphene (BNG) and nanochanneled and poly(diallyldimethylammonium chloride) PDDA-mediated RGO (nc-PDDA-Gr). [c]

tetraethylammonium tetrafluoroborate in anhydrous propylene carbonate (Et_4NBF_4/PC) and poly(ethylene glycol) diacrylate with 1-ethyl-3-methylimidazolium bis(trifluoromethylsulfonyl) imide (Ionogel electrolyte). [d] Please note that the data is based on the information found in the references and some of the values are calculated from the reported data. [e] References are listed in the main text. * The values were calculated from the corresponding references.